Letter

Experimental determination of the $E2$-$M1$ polarizability of the strontium clock transition

S. Dörscher, J. Klose, S. Maratha Palli,[*] and Ch. Lisdat[†]

Physikalisch-Technische Bundesanstalt, Bundesallee 100, 38116 Braunschweig, Germany

To operate an optical lattice clock at a fractional uncertainty below 10^{-17}, one must typically consider not only electric-dipole ($E1$) interaction between an atom and the lattice light field when characterizing the resulting lattice light shift of the clock transition but also higher-order multipole contributions, such as electric-quadrupole ($E2$) and magnetic-dipole ($M1$) interactions. However, strongly incompatible values have been reported for the $E2$-$M1$ polarizability difference of the clock states $(5s5p)\,{}^3P_0$ and $(5s^2)\,{}^1S_0$ of strontium [Ushijima *et al.*, Phys. Rev. Lett. **121**, 263202 (2018); Porsev *et al.*, Phys. Rev. Lett. **120**, 063204 (2018); Wu *et al.*, Phys. Rev. A **100**, 042514 (2019)]. This largely precludes operating strontium clocks with uncertainties of a few 10^{-18}, as the resulting lattice light shift corrections deviate by up to 1×10^{-17} from each other at typical trap depths. We have measured the $E2$-$M1$ light shift coefficient using our ^{87}Sr lattice clock and find a value of $\Delta\alpha_{\mathrm{qm}} = -987^{+174}_{-223}\,\mu$Hz. This result is in very good agreement with the value reported by Ushijima *et al.* [Phys. Rev. Lett. **121**, 263202 (2018)].

The interaction between the optical lattice and the trapped atom plays an important role in optical clocks with neutral atoms and has been investigated in several publications: As the accuracy of optical lattice clocks increases, one must take into account not only the electric-dipole ($E1$) interaction between atom and laser field [1] but also higher-order multipole interactions and two-photon coupling [2–7]. In electric-dipole approximation, the lattice light shift on the clock transition cancels for all lattice depths if the lattice is operated at the magic wavelength [1], but the higher-order contributions render this general cancellation impossible. Lastly, the individual contributions to the lattice light shift depend intricately on the motional state of the individual atom and thus on the population distribution of the atoms in the lattice [4,5,8].

Although the description of the light shift as a function of lattice depth can be simplified [4], the necessary conditions require careful testing and are not met in many cases. In its general form, several atomic parameters need to be known accurately, including the difference of the polarizabilities by electric-quadrupole ($E2$) and magnetic-dipole ($M1$) coupling at the given lattice light frequency and polarization. The most accurate determinations of this atomic parameter for strontium lattice clocks have been reported by Ushijima *et al.* [5] using an experimental approach, where the different contributions to the lattice light shift are separated by their dependencies on the motional state of the atoms and on the lattice light intensity, and by Porsev *et al.* [6] based on atomic structure calculations. Worryingly, these two values are extremely incompatible with each other, as they differ by about 22 times their combined standard uncertainty.

Given this discrepancy, it becomes difficult at best to accurately correct for the lattice light shift at an uncertainty of a few 10^{-18} or less in units of the clock transition frequency (referred to as fractional units hereafter): Between the two determinations [5,6], the $E2$-$M1$ contribution to the lattice light shift differs by about 1×10^{-17} in fractional units under typical conditions, including a trap depth of around $100E_{\mathrm{r}}$, where $E_{\mathrm{r}} = h^2/(2m\lambda_{\mathrm{m}}^2)$ is the photon recoil energy at the lattice wavelength λ_{m} for an atom of mass m, regardless of which light shift model [4,5] is used (see Fig. 1). Even in the motional ground state, i.e., in the limit of zero temperature, the difference exceeds 3×10^{-18} for any reasonable [9,10] lattice depth. Hence, the discrepancy cannot be mitigated by operating at lower lattice depth or by preparing the atomic sample closer to the motional ground state, e.g., by cooling to subrecoil temperatures as demonstrated recently for ytterbium [11].

Here, we report on an independent experimental determination of the $E2$-$M1$ light shift coefficient $\Delta\alpha_{\mathrm{qm}}(\lambda_{\mathrm{m}})$ of the clock transition in neutral strontium (probed on the $m_F = \pm9/2$ and $\Delta m_F = 0$ transitions). Our measurement procedure follows an approach similar to the one presented in Ref. [5]. We measure the differential light shift between samples with different motional state distributions at a fixed lattice depth in an experimental apparatus that uses the same interrogation laser [12] as our previous system [13] and a vertically oriented, one-dimensional optical lattice. The procedure used to measure differential frequency shifts is similar to those described in previous publications [13–15]; i.e., we run two

———————————

[*]Present address: Active Fiber Systems GmbH, Ernst Ruska Ring 17, 07745 Jena, Germany.
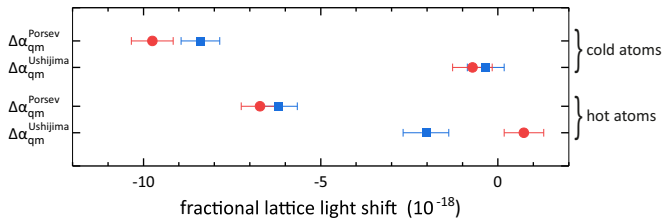
[†]christian.lisdat@ptb.de

FIG. 1. Lattice light shifts estimated using the value of the $E2$-$M1$ light shift coefficient $\Delta\alpha_{qm}$ reported by Porsev *et al.* [6] or by Ushijima *et al.* [5], respectively, for different models (dots: Ref. [4]; squares: Ref. [5]) and experimental conditions (see text) when the lattice light shift is equalized for trap depths of $77E_r$ and $149E_r$.

interleaved frequency stabilization loops with different experimental conditions in the same apparatus.

While Ushijima *et al.* [5] compared population distributions in the axial ground state and in the first excited motional state to increase the sensitivity to $\Delta\alpha_{qm}$, we induce the difference in motional state distribution by turning on or off selected cooling and filtering steps during preparation. Following transfer of the laser-cooled atoms from the second-stage magneto-optical trap into the optical lattice at a fixed depth of about $149E_r$, we either proceed to spectroscopy without further cooling and filtering or transfer atoms to lower-lying axial vibrational states by sideband cooling on the 689 nm ($\Delta F = 0$) transition and remove atoms in higher-lying vibrational states by reducing the trap depth to about $30E_r$ for several tens of ms before spectroscopy at a lattice depth of $149E_r$. The latter procedure is similar to the one described in Ref. [16] but uses a lower lattice depth due to the vertical orientation of the lattice beam. Overall, this results either in a nonthermal distribution near the axial motional ground state with strongly truncated high-energy tails in both the axial and radial degrees of freedom ("cold atoms") or in a nearly thermal distribution with substantially higher average energy in the external degrees of freedom ("hot atoms"). We observe a differential lattice light shift of $\Delta y(\text{hot} - \text{cold}) = 201(24)\times10^{-19}$; the instability of this measurement is shown in Fig. 2.

We combine this measurement with a second measurement using the "cold" motional state distribution at trap depths of $149E_r$ ("hi") and $77E_r$ ("lo") to separate the light shift's dependence on $\Delta\alpha_{qm}$ from its dependence on other atomic coefficients, in particular, on the $E1$ light shift coefficient $\Delta\alpha_{E1}$. We measure a differential light shift of $\Delta y(\text{hi} - \text{lo}) = -173(73) \times 10^{-20}$. Finally, we use sideband spectra on the clock transition (Fig. 3) to determine the lattice depth from the corner frequencies of the sidebands [17] and to characterize the vibrational state distribution (see below) in each case. We assign a fractional uncertainty of 5×10^{-2} to the lattice depth in order to account for potential errors, e.g., variations of the lattice intensity over time.

We require a model of the lattice light shift to interpret the measured light shifts and extract a value for $\Delta\alpha_{qm}$. We use the model reported in Ref. [4] as it accounts for the dependence on both the axial and the radial vibrational states and thus is well suited to describing the truncation of the population distribution, especially, but not only, in the low-temperature
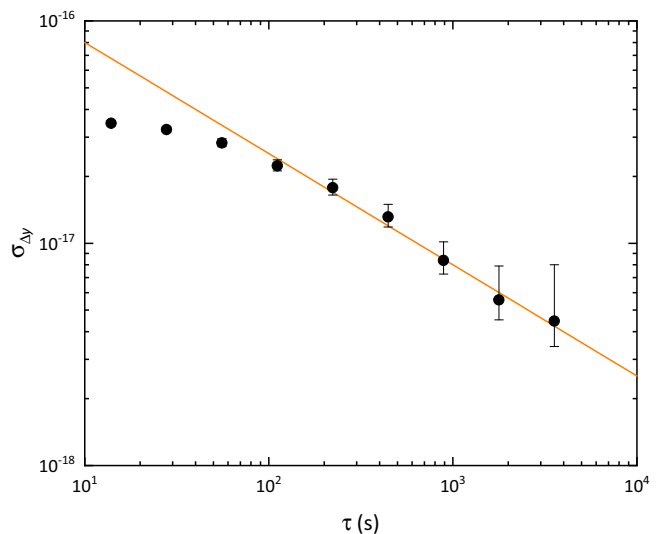

FIG. 2. Total Allan deviation of the measured differential lattice light shift between the high- and low-temperature configurations described in the main text. The line indicates an instability of $2.5\times10^{-16}/\sqrt{\tau(s)}$, where τ is the measurement time.

configuration. The light shift as a function of the lattice depth U in units of E_r is described by [4]

$$\delta\nu_{\text{clock}} = n_5\Delta\alpha_{qm} + [(n_1 + n_2)\Delta\alpha_{E1} - n_1\Delta\alpha_{qm}]U^{\frac{1}{2}}$$
$$- [\Delta\alpha_{E1} + (n_3 + n_4 + 4n_5)\Delta\beta]U$$
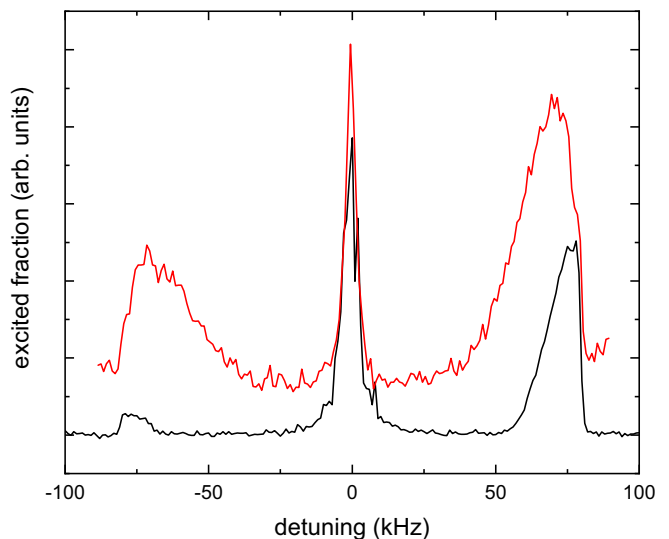$$+ [2\Delta\beta(n_1 + n_2)]U^{\frac{3}{2}} - \Delta\beta U^2. \quad (1)$$

FIG. 3. Sideband spectra recorded at a lattice depth of $149E_r$ with (lower trace) and without (upper trace) applying sideband cooling and truncating the population distribution. The smaller amplitude ratio of the red and blue sidebands as well as the much narrower width of the sidebands clearly show that atoms occupy lower motional states in the former case. We find axial (radial) temperatures of 2.1 μK (5.7 μK) for cold atoms and 6.6 μK (8.7 μK) for hot atoms. See the main text for further details. The curves are vertically offset for clarity.

The longitudinal (n_z) and the radial ($n_\rho = n_x + n_y$) motional quantum numbers contribute via the factors [4]

$$n_1 = (n_z + 1/2),$$
$$n_2 = [\sqrt{2}/(kw_0)](n_\rho + 1),$$
$$n_3 = (3/2)(n_z^2 + n_z + 1/2),$$
$$n_4 = \left[8/(3k^2w_0^2)\right](n_\rho^2 + 2n_\rho + 3/2), \quad \text{and}$$
$$n_5 = 1/(\sqrt{2}kw_0)(n_z + 1/2)(n_\rho + 1).$$

k and w_0 denote the wave number and waist radius of the lattice [18], respectively. Here, the light shift coefficients $\Delta\alpha_{qm}$, $\Delta\alpha_{E1}$, and $\Delta\beta$ are given in frequency units for convenience. They can be converted to their respective differential polarizabilities by multiplying $\Delta\alpha_{qm}$ and $\Delta\alpha_{E1}$ by $h\alpha_{E1}/E_r$ and $\Delta\beta$ by $h(\alpha_{E1}/E_r)^2$, where h is Planck's constant and α_{E1} is the $E1$ polarizability of either clock state at the magic wavelength [1]. We neglect a small traveling-wave term of the lattice light field in this work. The return loss of the lattice beam is estimated to be equal to the loss upon a single pass through the vacuum chamber of 4(2)%, from which we calculate a traveling-wave contribution to the trap depth of 1×10^{-4}. The reflected beam has been aligned by maximizing the power coupled back into the optical fiber delivering the lattice light to the physics package. We treat the radial degrees of freedom using the density of states given by Eq. (3) of Ref. [8] for any given n_z, i.e., in the approximations of a dense energy spectrum in the radial quantum numbers n_ρ and l and of a harmonic trapping potential.

We model the population distribution in each case by Boltzmann distributions with effective radial and axial temperatures (see Fig. 3). The former is derived from the shape of the respective sideband spectrum, shown in Fig. 3, using the formalism of Ref. [17], while the latter is adjusted such that the fraction of atoms in the axial vibrational ground state matches the observed ratio between the red and blue sideband amplitudes, taking into account the finite trap depth. For cold atoms, the radial energy distributions for each axial vibrational state are truncated according to the reduced trap depth that is applied during preparation. The mean values of n_1 through n_5 are then computed from these population distributions.

For the hyperpolarizability, the weighted average $\Delta\beta = 458(14)$ nHz of the light shift coefficients reported in Refs. [3,5–7,19,20] is used. This leaves only $\Delta\alpha_{E1}$ and $\Delta\alpha_{qm}$ as unknown parameters in Eq. (1). We can thus find the value of $\Delta\alpha_{qm}$ that allows a self-consistent description of our two measurement results by Eq. (1).

To estimate the uncertainty, we vary the most relevant input parameters within their uncertainties, derive the variations of $\Delta\alpha_{qm}$, and add these in quadrature. We mainly consider the largest sources of uncertainty, which are the determinations
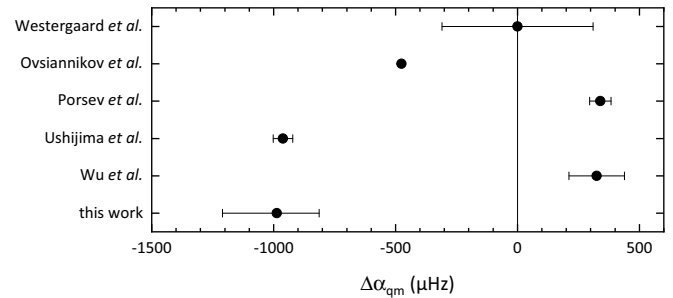

FIG. 4. Comparison of values reported for $\Delta\alpha_{qm}$ (Westergaard *et al.* [3], Ovsiannikov *et al.* [21], Porsev *et al.* [6], Ushijima *et al.* [5], Wu *et al.* [7]).

of the residual $E1$ light shift coefficient, $\Delta\alpha_{E1}$, and the temperature of the axial state distribution, i.e., the ratio of the sideband amplitudes, as well as the statistics of the light shift measurement between hot and cold atoms; other contributions are relatively small, including the uncertainty of the lattice depth.

We find

$$\Delta\alpha_{qm} = -987^{+174}_{-223} \,\mu\text{Hz}, \tag{2}$$

which is in excellent agreement with the measurement by Ushijima *et al.* [5], but differs from the values found by Porsev *et al.* [6] and Wu *et al.* [7], in the former case by more than seven times the combined standard uncertainty (Fig. 4).

In consequence, we discard the values from Refs. [6,7] and use the high-accuracy determination from Ref. [5]. Experimental [22] and theoretical [23] findings that have been reported by other groups recently are also in clear disagreement with the former. These results allow correcting the lattice light shift under typical conditions at a fractional uncertainty of 1×10^{-18} and better. Nevertheless, discrepancies remain between some of the results [5,22], albeit at a much smaller level than before. This highlights the need for further investigation of the differential $E2$-$M1$ polarizability.

The data that support the findings of this work are openly available in the Supplemental Material [24].

[1] H. Katori, K. Hashiguchi, E. Y. Il'inova, and V. D. Ovsiannikov, Magic Wavelength to Make Optical Lattice Clocks Insensitive to Atomic Motion, Phys. Rev. Lett. **103**, 153004 (2009).

[2] A. Brusch, R. Le Targat, X. Baillard, M. Fouché, and P. Lemonde, Hyperpolarizability Effects in a Sr Optical Lattice Clock, Phys. Rev. Lett. **96**, 103003 (2006).

[3] P. G. Westergaard, J. Lodewyck, L. Lorini, A. Lecallier, E. A. Burt, M. Zawada, J. Millo, and P. Lemonde, Lattice-Induced Frequency Shifts in Sr Optical Lattice Clocks at the 10^{-17} Level, Phys. Rev. Lett. **106**, 210801 (2011).

[4] R. C. Brown, N. B. Phillips, K. Beloy, W. F. McGrew, M. Schioppo, R. J. Fasano, G. Milani, X. Zhang, N. Hinkley, H. Leopardi, T. H. Yoon, D. Nicolodi, T. M. Fortier, and A. D. Ludlow, Hyperpolarizability and Operational Magic Wavelength in an Optical Lattice Clock, Phys. Rev. Lett. **119**, 253001 (2017).

[5] I. Ushijima, M. Takamoto, and H. Katori, Operational Magic Intensity for Sr Optical Lattice Clocks, Phys. Rev. Lett. **121**, 263202 (2018).

[6] S. G. Porsev, M. S. Safronova, U. I. Safronova, and M. G. Kozlov, Multipolar Polarizabilities and Hyperpolarizabilities in the Sr Optical Lattice Clock, Phys. Rev. Lett. **120**, 063204 (2018).

[7] F.-F. Wu, Y.-B. Tang, T.-Y. Shi, and L.-Y. Tang, Dynamic multipolar polarizabilities and hyperpolarizabilities of the Sr lattice clock, Phys. Rev. A **100**, 042514 (2019).

[8] K. Beloy, W. F. McGrew, X. Zhang, D. Nicolodi, R. J. Fasano, Y. S. Hassan, R. C. Brown, and A. D. Ludlow, Modeling motional energy spectra and lattice light shifts in optical lattice clocks, Phys. Rev. A **101**, 053416 (2020).

[9] P. Lemonde and P. Wolf, Optical lattice clock with atoms confined in a shallow trap, Phys. Rev. A **72**, 033409 (2005).

[10] A. Aeppli, A. Chu, T. Bothwell, C. J. Kennedy, D. Kedar, P. He, A. M. Rey, and J. Ye, Hamiltonian engineering of spin-orbit–coupled fermions in a Wannier-Stark optical lattice clock, Sci. Adv. **8**, eadc9242 (2022).

[11] X. Zhang, K. Beloy, Y. S. Hassan, W. F. McGrew, C.-C. Chen, J. L. Siegel, T. Grogan, and A. D. Ludlow, Subrecoil Clock-Transition Laser Cooling Enabling Shallow Optical Lattice Clocks, Phys. Rev. Lett. **129**, 113202 (2022).

[12] S. Häfner, S. Falke, C. Grebing, S. Vogt, T. Legero, M. Merimaa, C. Lisdat, and U. Sterr, 8×10^{-17} fractional laser frequency instability with a long room-temperature cavity, Opt. Lett. **40**, 2112 (2015).

[13] R. Schwarz, S. Dörscher, A. Al-Masoudi, E. Benkler, T. Legero, U. Sterr, S. Weyers, J. Rahm, B. Lipphardt, and C. Lisdat, Long term measurement of the ^{87}Sr clock frequency at the limit of primary Cs clocks, Phys. Rev. Res. **2**, 033242 (2020).

[14] S. Falke, N. Lemke, C. Grebing, B. Lipphardt, S. Weyers, V. Gerginov, N. Huntemann, C. Hagemann, A. Al-Masoudi, S. Häfner, S. Vogt, U. Sterr, and C. Lisdat, A strontium lattice clock with 3×10^{-17} inaccuracy and its frequency, New J. Phys. **16**, 073023 (2014).

[15] A. Al-Masoudi, S. Dörscher, S. Häfner, U. Sterr, and C. Lisdat, Noise and instability of an optical lattice clock, Phys. Rev. A **92**, 063814 (2015).

[16] S. Dörscher, R. Schwarz, A. Al-Masoudi, S. Falke, U. Sterr, and C. Lisdat, Lattice-induced photon scattering in an optical lattice clock, Phys. Rev. A **97**, 063419 (2018).

[17] S. Blatt, J. W. Thomsen, G. K. Campbell, A. D. Ludlow, M. D. Swallows, M. J. Martin, M. M. Boyd, and J. Ye, Rabi spectroscopy and excitation inhomogeneity in a one-dimensional optical lattice clock, Phys. Rev. A **80**, 052703 (2009).

[18] A waist radius of about 65 μm has been measured for our lattice, using a beam-profiling camera. The determination of $\Delta\alpha_{\mathrm{qm}}$ depends only weakly on this parameter, however: For a thermal distribution, $\langle n_\rho^j \rangle_{\mathrm{th}} \approx \langle E_\rho^j \rangle_{\mathrm{th}} / (h\nu_\rho)^j$, where $\langle\rangle_{\mathrm{th}}$ denotes averaging over the distribution, with the average of the jth power of the radial energy $\langle E_\rho^j \rangle_{\mathrm{th}}$ being independent of w_0 and $\nu_\rho / \nu_z \propto k w_0$ [17]. Regarding n_4, $\langle n_\rho^2 \rangle_{\mathrm{th}} \gg 2 \langle n_\rho \rangle_{\mathrm{th}}$, since both $\sqrt{\langle n_\rho^2 \rangle_{\mathrm{th}}}$ and $\langle n_\rho \rangle_{\mathrm{th}}$ are about 500 or larger in our case. The factors $(k w_0)^j$ in n_2, n_4, and n_5 of Eq. (1) are thus canceled by those resulting from $\langle n_\rho^j \rangle_{\mathrm{th}}$ in good approximation.

[19] R. Le Targat, L. Lorini, Y. Le Coq, M. Zawada, J. Guéna, M. Abgrall, M. Gurov, P. Rosenbusch, D. G. Rovera, B. Nagórny, R. Gartman, P. G. Westergaard, M. E. Tobar, M. Lours, G. Santarelli, A. Clairon, S. Bize, P. Laurent, P. Lemonde, and J. Lodewyck, Experimental realization of an optical second with strontium lattice clocks, Nat. Commun. **4**, 2109 (2013).

[20] T. L. Nicholson, S. L. Campbell, R. B. Hutson, G. E. Marti, B. J. Bloom, R. L. McNally, W. Zhang, M. D. Barrett, M. S. Safronova, G. F. Strouse, W. L. Tew, and J. Ye, Systematic evaluation of an atomic clock at 2×10^{-18} total uncertainty, Nat. Commun. **6**, 6896 (2015).

[21] V. D. Ovsiannikov, S. I. Marmo, V. G. Palchikov, and H. Katori, Higher-order effects on the precision of clocks of neutral atoms in optical lattices, Phys. Rev. A **93**, 043420 (2016).

[22] K. Kim, A. Aeppli, T. Bothwell, and J. Ye, Evaluation of lattice light shift at mid 10^{-19} uncertainty for a shallow lattice Sr optical clock, arXiv:2210.16374

[23] F.-F. Wu, T.-Y. Shi, and L.-Y. Tang, Contributions of negative-energy states to the E2-M1 polarizability of the Sr clock, arXiv:2301.06740.

[24] See Supplemental Material at http://link.aps.org/supplemental/10.1103/PhysRevResearch.5.L012013 for data that support the findings of this work.